

EFFECTS OF DIFFRACTION ON THE MEASUREMENT OF THE ACOUSTIC PROPERTIES OF LIQUIDS IN THIN-WALLED CONTAINERS

Gregory Kaduchak and Dipen N. Sinha
Los Alamos National Laboratory, MS D429, Los Alamos NM 87545

Abstract - A simple method which does not require calibration with a reference liquid for the determination of attenuation and density of a fluid contained within a thin-walled cell is demonstrated. The method relies on temporally filtering the impulse response of the system to partially deconvolve the transfer function associated with the wall. Experiments are conducted on cells of differing material construction and wall thickness which demonstrate the effectiveness of this method in obtaining accurate *near-field* measurements of density and attenuation.

I. Introduction

There are many applications where direct contact with a fluid is not possible and it is necessary to acoustically probe a fluid through the wall of a container.¹ This is extremely important when the liquids are extremely toxic or hazardous. It is often the case that such liquid samples are small requiring measurements to be conducted in containers with small length scales. This constrains measurements to be performed in the near field of the exciting/receiving transducers. The present research defines a frequency domain technique which may be used to gain reliable attenuation and density measurements of liquids in thin-walled containers where the measurements are well within the near-field transition region of the exciting/receiving transducers.

II. Near Field in Thin Walled Containers

The near field of a circular piston transducer is a complicated diffraction pattern with spatially varying pressure distributions.²⁻⁴ It is defined by a focusing event (caustic) which results in a large amplitude pressure variation along the axis of the transducer. To demonstrate the complexity of this region, the near-field pattern for a .25" transducer radiating into isopropanol at 4 MHz is shown in Fig. 1(a). The near field transition region is defined by the point A. This

marks the transition between near-field and far-field beam spreading.

Figure 1(b) displays the diffraction pattern when a glass wall is placed between the transducer and the fluid medium. The calculation is performed using standard propagation integrals which rely on a Huygens reconstruction of the propagating wavefronts. For simplicity, only compressional waves are considered important and reverberation within the wall is ignored. (The effect of the wall reverberation is neglected since the measurement technique described below is used to temporally isolate the echoes in the reverberation signature.) Note that in the wall region, the pattern is contracted in length, which results in shortening the near field

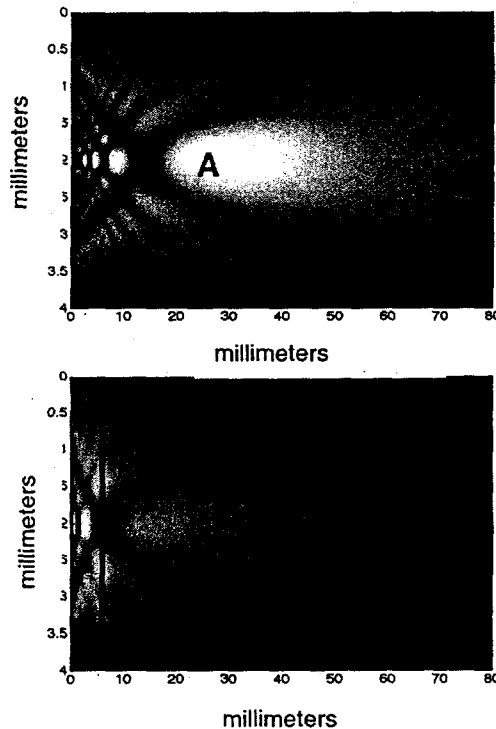


Figure 1 - (a) Near field pattern in fluid. (b) Near field pattern with wall inserted between transducer and fluid. Wall thickness h is 7 mm.

DISCLAIMER

This report was prepared as an account of work sponsored by an agency of the United States Government. Neither the United States Government nor any agency thereof, nor any of their employees, make any warranty, express or implied, or assumes any legal liability or responsibility for the accuracy, completeness, or usefulness of any information, apparatus, product, or process disclosed, or represents that its use would not infringe privately owned rights. Reference herein to any specific commercial product, process, or service by trade name, trademark, manufacturer, or otherwise does not necessarily constitute or imply its endorsement, recommendation, or favoring by the United States Government or any agency thereof. The views and opinions of authors expressed herein do not necessarily state or reflect those of the United States Government or any agency thereof.

DISCLAIMER

**Portions of this document may be illegible
in electronic image products. Images are
produced from the best available original
document.**

region. The contraction is a result of the sound speed in the wall material being much greater than the fluid implying a longer wavelength in the wall.

III. Frequency response and impulse response of a thin-walled container

Consider the thin-walled cell displayed in Fig. 2. It consists of two parallel walls each attached to a transducer. The measured frequency spectrum for a cell constructed with glass walls of thickness $h = 1.2$ mm and a path length $L = 10$ mm is shown in Fig. 3(a). The spectrum is the result of the combined effect of resonances which are set up in the wall material and the fluid. The closely spaced resonance peaks are associated with resonances in the liquid and their spacing scales with the cavity length L . The broader 'humps' (gray line) are associated with resonances within the cell walls and have a frequency spacing which scales with the wall thickness h .

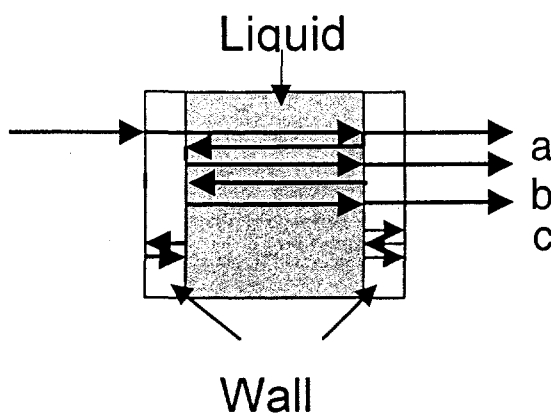


Figure 2 – Diagram for ray paths in a thin-walled cell.

The band-limited impulse response of the system (obtained by a Fourier transform of the data in Fig. 3(a)) is displayed in Fig. 3(b). There are multiple groups of impulses (a and b). Each group contains multiple echoes that result from a single pulse undergoing multiple reflections within the wall boundaries. The first group corresponds to echoes traversing the ray path a shown in Fig. 2 and the second group corresponds to echoes traversing the ray path b. By assuring that the bandwidth B of the measured data obeys the condition

$$\frac{1}{B} \leq \frac{h}{c_w}$$

where c_w is the compressional wave speed of the wall material, the impulses reverberant within the wall may be temporally isolated.

The ability to temporally isolate the reverberant echoes within the wall is very useful in that it is possible to partially deconvolve the wall response of the system by choosing only the returns of interest. The technique presented here requires choosing only the first impulse in the first group (labeled a) and the first impulse in the second group (labeled b) to obtain a good approximation of the attenuation and density of the fluid contained in the closed cell.

It should be noted that making stepped frequency measurements and collecting the quadrature sampled data in the frequency domain and transforming into the time domain results in a time signature with a much higher signal to noise ratio than obtained in a standard pulse-echo measurement. This is due to the fact that in a pulse-echo measurement, energy is spread over the entire frequency range as opposed to excitation with a single frequency. This is akin to the

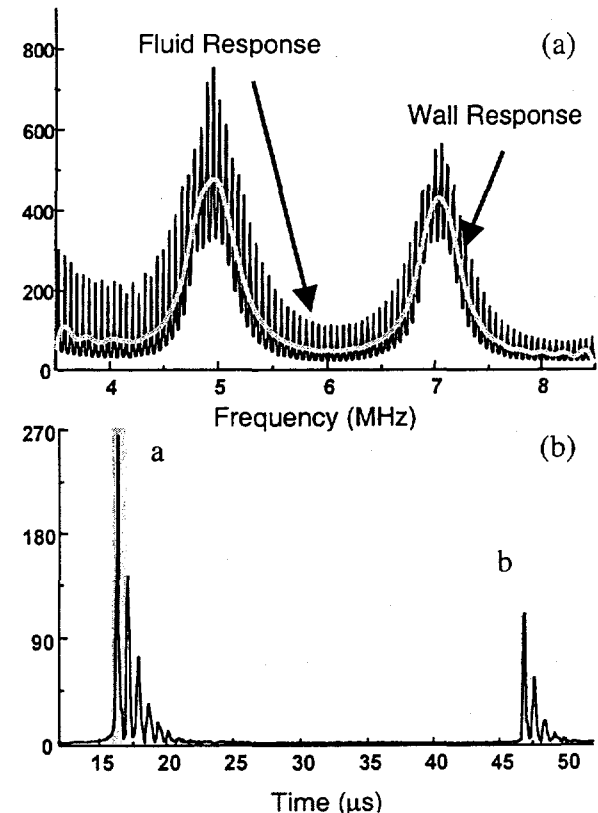


Figure 3 – (a) Measured spectrum. (b) Impulse response from FFT of (a).

RECEIVED
DEC 13 2000
OSTI

large singnal to noise gains encountered with pulse compression techniques used in sonar and radar applications.

IV. Method of calculation

The attenuation and density of the fluid in the cell may be calculated by temporally filtering the first impulse (labeled a) in the first group and the first impulse (labeled b) in the second group from the impulse response shown in Fig. 3(b). These pulses refer to disturbances that traverse the thickness of each wall only once and traverse the cavity one or three times, respectively. By calculating the spectrum of the isolated pulses (using a Fourier transform), the ratio of the spectral amplitudes is given by

$$\frac{\text{spectrum(pulse } b)}{\text{spectrum(pulse } a)} = \frac{R^2 e^{-\alpha 3L f^2}}{e^{-\alpha L f^2}}$$

where a frequency squared dependence is assumed for the attenuation of the liquid. The unknown quantities are the attenuation coefficient α and the reflection coefficient R of the fluid-wall interface. (All other transmission coefficients which are common to both pulses cancel.) Taking the natural logarithm of this equation yields

$$\ln\left(\frac{\text{spectrum(pulse } b)}{\text{spectrum(pulse } a)}\right) = -2\alpha L f^2 + \ln(R^2).$$

The right hand side of the equation is a straight line as a function of f^2 with a slope proportional to the attenuation of the liquid and the reflection coefficient (which is proportional to the impedance of the wall and liquid) contained in the y intercept. The \ln of the spectral ratio is plotted in Fig. 4 for measurements made on isopropanol in the cell defined in the previous section.

V. Near field diffraction effects

It is important to note how the near-field diffraction effects are manifest in the measurement shown in Fig. 4. Figure 5 displays the near-field distance as a function of frequency for a .25" diameter transducer attached to the cell walls. (The same type used to make the measurement.) The values plotted are

corrected for the presence of the wall material. As the frequency increases, so does the extent of the near-field.

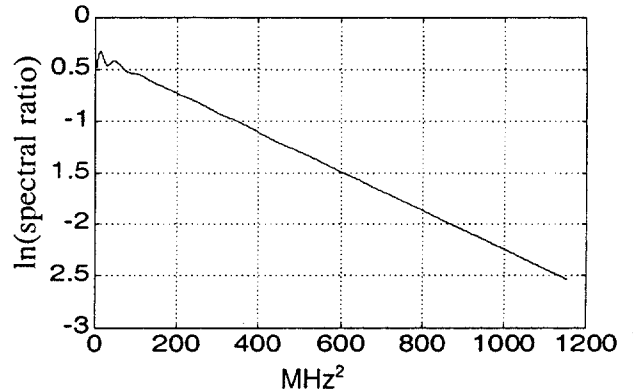


Figure 4 – Natural Logarithm of the spectral amplitudes of pulses a and b.

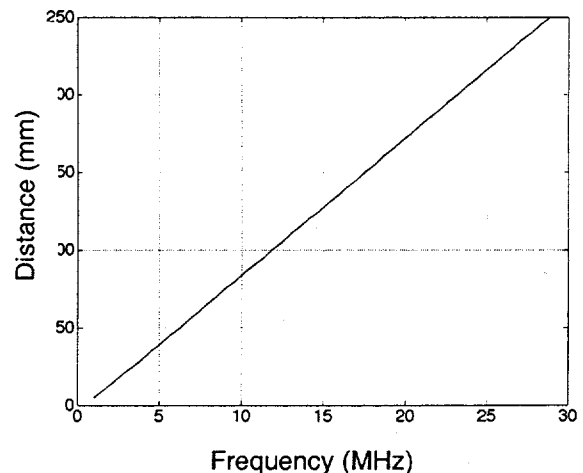


Figure 5 – Near field distance for a thin-walled cell.

The method described above to calculate the attenuation and density of the liquid is applied to data generated from diffraction calculations for this cell. The cell contains a hypothetical fluid with no attenuation and the reflection coefficient at the fluid-wall boundary is set to unity for simplicity. (All losses should thus be associated with diffraction.) Figure 6(a) displays the log of the spectral ratio corresponding to pulses a and b. The lines displayed are fairly flat (zero slope) as a function of frequency yielding an attenuation of zero (as expected). Note at lower frequencies there are appreciable slope variations that would lead to erroneous attenuation results if the measurements were bandwidth limited to those frequency ranges. It is interesting that these

imperfections occur when the pulses are closest to the near field transition boundary (especially pulse b). Also, it should be noted that the value of the y intercept is not zero. This implies a frequency independent loss mechanism associated with diffraction.

Figure 6(b) displays the same calculation as above except a representative value of attenuation and impedance are given to the liquid (isopropanol) in the cell. Beyond the low frequency range, it appears that the slope of the lines are fairly constant implying reliable attenuation measurements well within the near-field transition range. (The values on the y axis have been shifted down for clarity.)

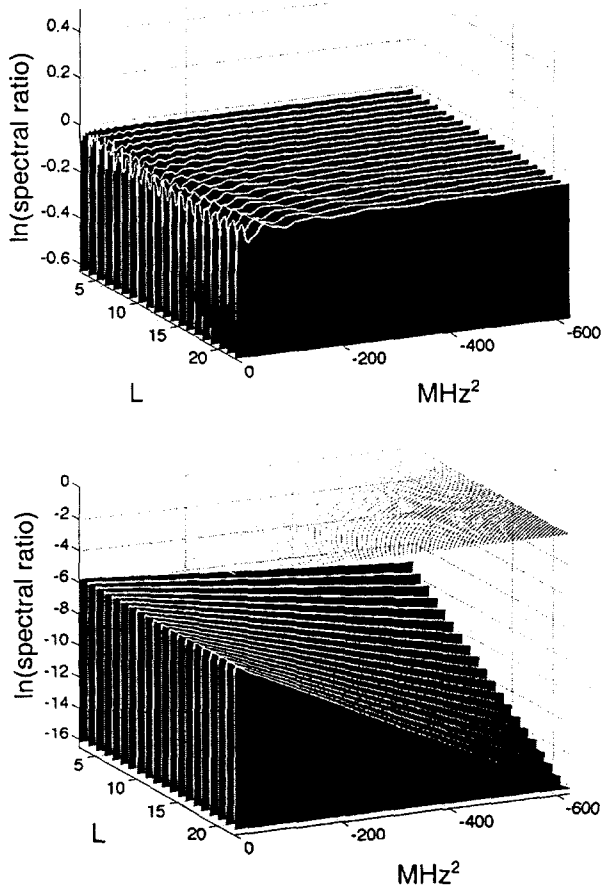


Figure 6 – (a) Walled cell containing a fluid with no attenuation. (b) Same walled cell containing a fluid with attenuation

VI. Experiments and Results

Experiments were conducted with cells of differing material construction, wall thickness h , and cavity length L . They are defined in Table I. They all contained isopropanol as the test fluid. The transducers are .25" in diameter with a center frequency of 30 MHz. Figure 6(a) displays theoretical predictions using scalar diffraction theory and passing the results through the aforementioned calculation technique. Figure 6(b) displays the experimental results. The measurements compare extremely well with literature values:

Attenuation (α): $9.0 \text{ Np}/(\text{m MHz}^2)$ Literature
 $9.3 \pm 0.05 \text{ Np}/(\text{m MHz}^2)$ Experiment

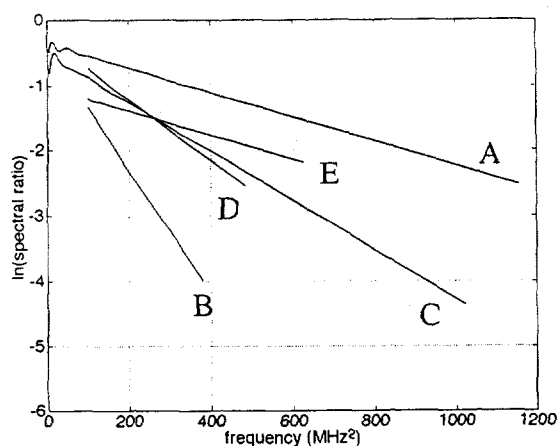
Density: 800 kg/m^3 Literature
 $850 \pm 0.6 \text{ kg/m}^3$ Experiment

Table I – Cell Properties

Material	Wall Thickness (mm)	Cell Length (mm)
A Quartz	1.2	10
B Quartz	1.2	50
C Aluminum	2.5	10
D SS304	2.0	25
E Glass	1.2	20

VII. Summary

An approach was presented whereby physical properties of liquids, such as sound attenuation and density, can be measured noninvasively in thin-walled containers. These measurements are done entirely in the near-field region using a frequency-technique. By converting the frequency-domain information into the time domain, it is possible to deconvolve the wall effects by temporally filtering the band-limited impulse response. It is shown that near-field diffraction corrections, away from the transition region, appear to be small and thus do not have a large affect on the measurements. Measurements of liquids in thin-walled cells made from various materials and with different path lengths demonstrate the robustness of this approach. It is important to note that this approach does not require calibration using reference liquids.



[4] H. Seki, A. Granato, and R. Truell, "Diffraction effects in the ultrasonic field of a piston source and their importance in the accurate measurement of attenuation," *J. Acoust. Soc. Am.* **28**, 230-238 (1956).

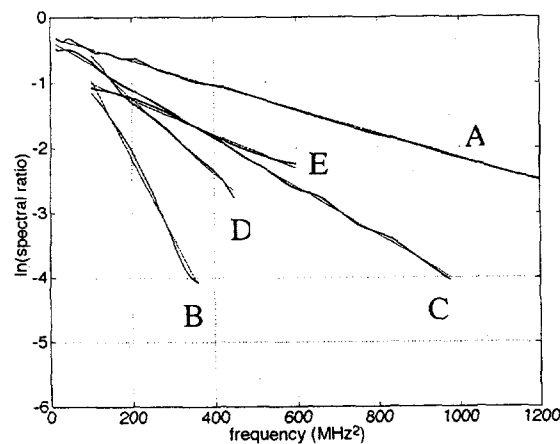


Figure 7 – (a) Theoretical predictions for the log of the spectral amplitude. (b) Experimental results.

VII. References

- [1] D. N. Sinha and G. Kaduchak, "Noninvasive determination of sound speed and attenuation in chemical warfare agents," in *Handbook of Elastic Properties of Solids, Liquids, and Gases*, ed. By D. Sinha and M. Levy (Academic, New York, 2000).
- [2] C. J. Daly and N. A. H. K. Rao, "The arccos and Lommel formulations-Approximate closed-form diffraction corrections," *J. Acoust. Soc. Am.* **105**, 3067-3077 (1999).
- [3] W. Xu and J. Kaufman, "Diffraction correction methods for insertion ultrasound attenuation estimation," *IEEE Trans. Biomed. Eng.* **40**, 563-569 (1993).